JOURNAL OF NATURAL PRODUCTS

Article

pubs.acs.org/jnp

Inhibition of TNF-α-Induced Inflammation by Andrographolide via Down-Regulation of the PI3K/Akt Signaling Pathway

Haw-Wen Chen,[†] Ai-Hsuan Lin,[‡] Hsing-Chin Chu,[‡] Chien-Chun Li,[‡] Chia-Wen Tsai,[†] Che-Yi Chao,[§] Chau-Jong Wang,[⊥] Chong-Kuei Lii,*[,†] and Kai-Li Liu*[,‡,∥]

[†]Department of Nutrition, China Medical University, Taichung 404, Taiwan, Republic of China

[‡]Department of Nutrition, Chung Shan Medical University, Taichung 402, Taiwan, Republic of China

[§]Department of Health and Nutritional Biotechnology, Asia University, Taichung 413, Taiwan, Republic of China

[⊥]Institute of Biochemistry and Biotechnology, Chung Shan Medical University, Taichung 402, Taiwan, Republic of China

[∥]Department of Dietitian, Chung Shan Medical University Hospital, Taichung 402, Taiwan, Republic of China

Supporting Information

ABSTRACT: Andrographolide (**1**), an active constituent of *Andrographis paniculata,* decreased tumor necrosis factor-α (TNF-α)-induced intercellular adhesion molecule-1 (ICAM-1) expression and adhesion of HL-60 cells onto human umbilical vein endothelial cells (HUVEC), which are associated with inflammatory diseases. Moreover, **1** abolished TNF-α-induced Akt phosphorylation. Transfection of an activated Akt1 cDNA vector increased Akt phosphorylation and ICAM-1 expression like TNF-α. In addition, **1** and LY294002 blocked TNF-α-induced IκB-α degradation and nuclear p65 protein accumulation, as well as the DNA-binding activity of NF-κB. Compound **1** exhibits anti-inflammatory properties through the inhibition of TNF-α-induced ICAM-1 expression. The anti-inflammatory activity of **1** may be associated with the inhibition of the PI3K/Akt pathway and downstream target NF-κB activation in HUVEC cells.

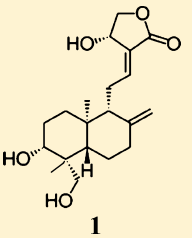

1

Inflammation, an essential factor in many chronic diseases, is caused by various stimuli, such as tumor necrosis factor-α (TNF-α), interleukin-1β, and interferon-γ (INF-γ).[1−3] Atherosclerosis is a type of chronic inflammatory vascular disease. Considerable efforts have been made to identify the essential role of adhesion molecule up-regulation in vascular diseases.[4] ICAM-1, a cell surface glycoprotein that belongs to the immunoglobulin supergene family, is important in mediating leukocyte adhesion, arrest, and transmigration to blood vessels at the inflammatory site.[5] In apo E-deficient mice, deletion of ICAM-1 gene expression causes significant reduction of atherosclerotic lesions.[6] A previous study has demonstrated that the plasma level of ICAM-1 is a new predictor of atherosclerotic risk.[7] In this regard, the modulation of ICAM-1 expression could be a therapeutic strategy against atherosclerosis and inflammation-related diseases.

TNF-α, commonly released by macrophages in atherosclerotic lesions, provides cell signals to induce inflammatory responses in endothelial cells through activation of nuclear factor-κB (NF-κB).[8,9] NF-κB is composed of homodimers or heterodimers of members of the *Rel* family, and the dimer is retained in an inactive form in the cytoplasm by binding to the inhibitory subunit IκB-α.[10] In response to external stimuli, the proteasome-dependent degradation of IκB-α through IκB kinase is initiated, which results in NF-κB activation.[11] The freed NF-κB is then translocated to the cell nucleus, where it binds to a κB enhancer element and stimulates the transcription of target genes.[8,9,12] Activated NF-κB has been recognized in human atherosclerotic plaques, and the induction of NF-κB-dependent gene expression is required for development of atherosclerosis.[13,14]

The phosphatidylinositol 3-kinase (PI3K)/Akt signaling pathway is reportedly involved in various cellular processes, including cell cycle progression, proliferation, and survival in response to extracellular stimuli.[15] Study data have shown that activation of PI3K and its downstream target Akt is essential for TNF-α-induced NF-κB activation.[16] Moreover, the PI3K signaling pathway plays a crucial role in monocyte recruitment, which is linked to the development of several vascular diseases.[17] The potent PI3K inhibitor PIK-75 decreased TNF-α-induced adhesion molecule expression and monocyte adhesion in human umbilical vein endothelial cells (HUVEC).[18] Accumulating results have demonstrated that phytochemicals such as kahweol, apigenin, and luteolin, through inhibition of the PI3K/Akt pathway, reduce inflammatory responses in endothelial cells.[19,20]

Andrographis paniculata (Burm. f.) Nees (Acanthaceae) is used as a traditional Chinese herbal medicine and is cultivated widely and used in various Asian countries. Andrographolide (**1**), a major constituent of *A. paniculata*, accounts for 3% of the dried leaves at 120 days after sowing.[21] Compound **1** has numerous reported pharmacological properties and has been used extensively clinically for the treatment of infections, inflammation, colds, fever, and diarrhea and as an antidote for snakebites.[22] The anti-inflammatory activities of *A. paniculata*

Received: July 27, 2011
Published: October 25, 2011

and **1** have been studied thoroughly.[23,24] Since anti-inflammatory action has been considered as a therapeutic strategy for the treatment of atherosclerosis,[25,26] it has been shown that **1** decreases TNF-α-induced ICAM-1 expression and monocyte adhesion in EA.hy926 human endothelial cells.[27,28] The present study was designed to investigate whether or not the reduction of TNF-α-induced ICAM-1 expression in HUVEC cells by **1** is related to the inhibition of the PI3K/Akt pathway and downstream target NF-κB activation.

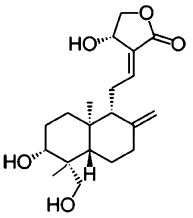

1

RESULTS AND DISCUSSION

Cell Viability. After treatment with andrographolide (**1**), the cytotoxicity to HUVEC cells was measured using the 3-(4,5-dimethylthiazol-2yl)-2,5-diphenyltetrazolium bromide (MTT) assay. The cell viabilities of these cells treated with TNF-α alone or with TNF-α and 5, 10, or 20 μM **1** were 103.8 ± 6.1%, 96.4 ± 1.9%, 94.6 ± 4.3%, and 87.5 ± 3.5%, respectively, compared with the unstimulated controls (100%). Thus, the inhibitory activity of **1** on TNF-α-induced events in HUVEC cells was not the result of cytotoxic effects.

HL-60 Cell Adhesion and ICAM-1 Protein Expression by Andrographolide (1) in TNF-α-Stimulated HUVEC Cells. Incubation of confluent HUVEC cells with 1 ng/mL TNF-α for 6 h resulted in a 6-fold increase in the number of adherent HL-60 cells compared with the unstimulated controls. This increase in HL-60 cell adhesion was suppressed considerably by pretreatment of the HUVEC cells with **1** for 16 h. The highest dose of **1** tested (20 μM) inhibited the stimulated adhesion by about 73% (Figure 1). Treatment with andrographolide (**1**) alone did not induce HL-60 cell adhesion and ICAM-1 expression (data not shown).

It has been shown that the cell adhesion molecules expressed in endothelial cells are required for monocyte and T-cell adhesion onto endothelial cells.[29] As **1** inhibited TNF-α-induced HL-60 cell adhesion onto HUVEC cells, the effect of andrographolide (**1**) was examined on TNF-α-induced ICAM-1 expression. Treatment of these cells with 1 ng/mL TNF-α for 6 h increased total and cell surface ICAM-1 expression substantially as assessed by Western blot analysis and flow cytometry, respectively. Pretreatment of HUVEC cells with **1** for 16 h significantly reduced TNF-α-induced total and cell surface ICAM-1 expression (Figure 2A and B; $p < 0.05$).

It has been demonstrated that andrographolide (**1**) decreases the expression of lipopolysaccharide (LPS)/IFN-γ-induced inducible nitric oxide synthase and matrix metalloproteinase (MMP) 9 in rat vascular smooth muscle cells and attenuates neointimal formation in balloon-injured rat carotid arteries.[30] In agreement with the cardiovascular protective potential of **1**, a previous study has shown that **1** decreased TNF-α-induced ICAM-1 expression in EA.hy926 cells through the induction of heme oxygenase 1 (HO-1) expression.[27]

ICAM-1 mRNA Expression and ICAM-1 Promoter Activity by Andrographolide (1) in TNF-α-Stimulated HUVEC Cells. RT-PCR was performed to clarify whether or not down-regulated ICAM-1 expression by **1** is controlled at the transcriptional level. As shown in Figure 3A, pretreatment with **1** suppressed TNF-α-induced ICAM-1 mRNA expression significantly. When a luciferase reporter construct containing the human ICAM-1 promoter region was transfected transiently into HUVEC cells, the promoter activity of ICAM-1 was increased significantly in response to TNF-α. This increased activity was reduced by pretreatment with 20 μM **1** (Figure 3B).

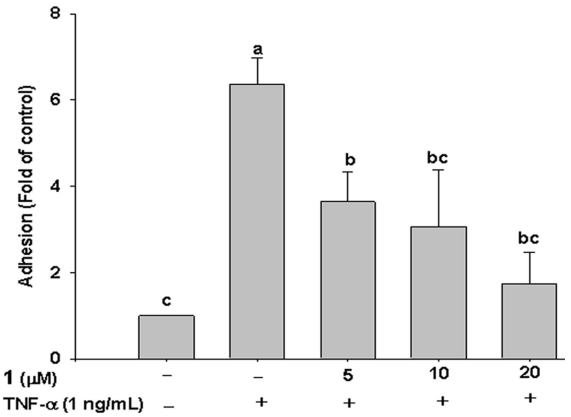

Figure 1. Effect of andrographolide (**1**) on TNF-α-induced HL-60 cell adhesion. Cells were pretreated with 5 to 20 μM **1** for 16 h before being challenged with 1 ng/mL TNF-α for an additional 6 h. Cells were co-incubated with BCECF-AM-labeled HL-60 cells for 30 min, and then the adhesion was determined as described in the Experimental Section. Values are means ± SD of three independent experiments, and values not designated by the same letter are significantly different ($p < 0.05$).

ICAM-1 plays an important role in inflammatory vascular diseases because of its ability to enhance monocyte adhesion onto the endothelium in response to TNF-α or oxidized low-density lipoproteins.[31] In this regard, inhibition of abnormally induced ICAM-1 expression may have beneficial effects on cardiovascular disease. Glabridin, a flavonoid and a main constituent of nonpolar extracts of licorice, exhibits anti-inflammatory and antiatherosclerotic activity due to reduction of TPH-1 cell adhesion and ICAM-1 expression in TNF-α-stimulated HUVEC cells.[32] The present data demonstrate that treatment with **1** suppressed TNF-α-induced ICAM-1 expression significantly, as well as HL-60 adhesion onto HUVEC cells.

NF-κB Activation in TNF-α-Stimulated HUVEC Cells by Andrographolide (1). Given that the NF-κB signaling pathway plays a crucial role in TNF-α-induced ICAM-1 expression,[8] the effect of **1** on TNF-α-induced NF-κB activation was examined. On TNF-α treatment, the IκB-α protein disappeared from cytosolic fractions, whereas the amount of nuclear p65 protein increased considerably when compared with controls. Hence, the addition of **1** abolished the TNF-α-induced IκB-α degradation and nuclear p65 protein levels (Figure S1A, B; $p < 0.05$, Supporting Information), at the concentrations used.

EMSA experiments were further used to evaluate the effect of **1** on NF-κB activation (Figure S1C, Supporting Information). Treatment with TNF-α increased the DNA-binding activity of the NF-κB nuclear protein significantly. TNF-α-induced NF-κB nuclear protein−DNA binding activity was reduced markedly in cells pretreated with **1**. The specificity of NF-κB binding was

dx.doi.org/10.1021/np200631v | J. Nat. Prod. 2011, 74, 2408–2413

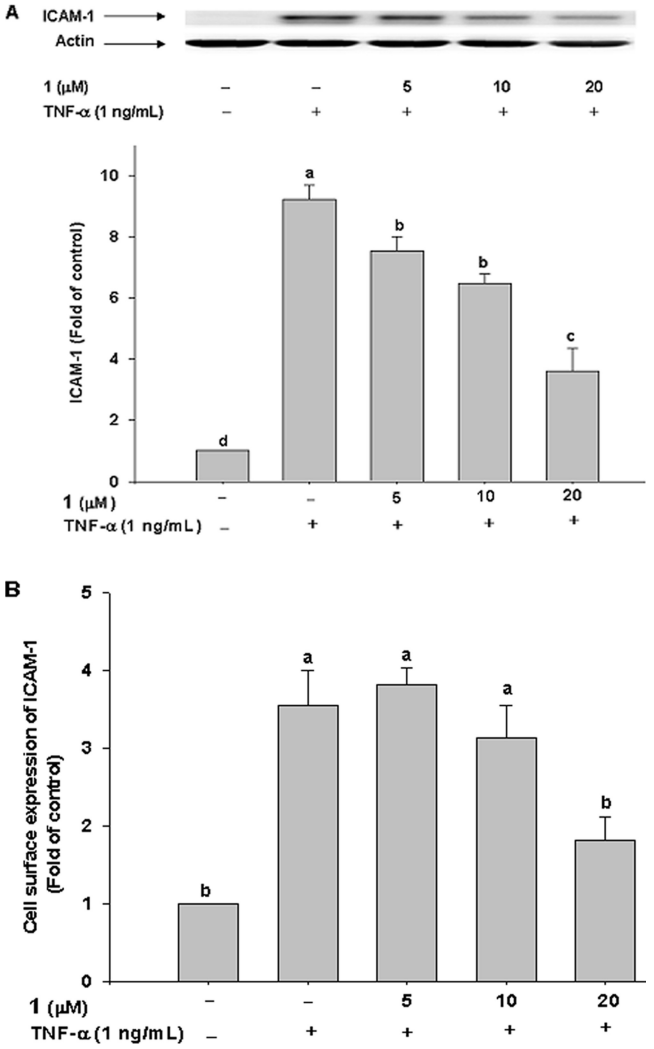

Figure 2. Effect of andrographolide (**1**) on ICAM-1 protein expression in TNF-α-stimulated HUVEC cells. Cells were pretreated with 5 to 20 μM **1** for 16 h before being challenged with 1 ng/mL TNF-α for an additional 6 h. Western blot analysis (A) and fluorescence flow cytometry (B) were used to measure the total cellular protein and cell surface protein of ICAM-1, respectively. Values are means ± SD of three independent experiments, and values not designated by the same letter are significantly different ($p < 0.05$).

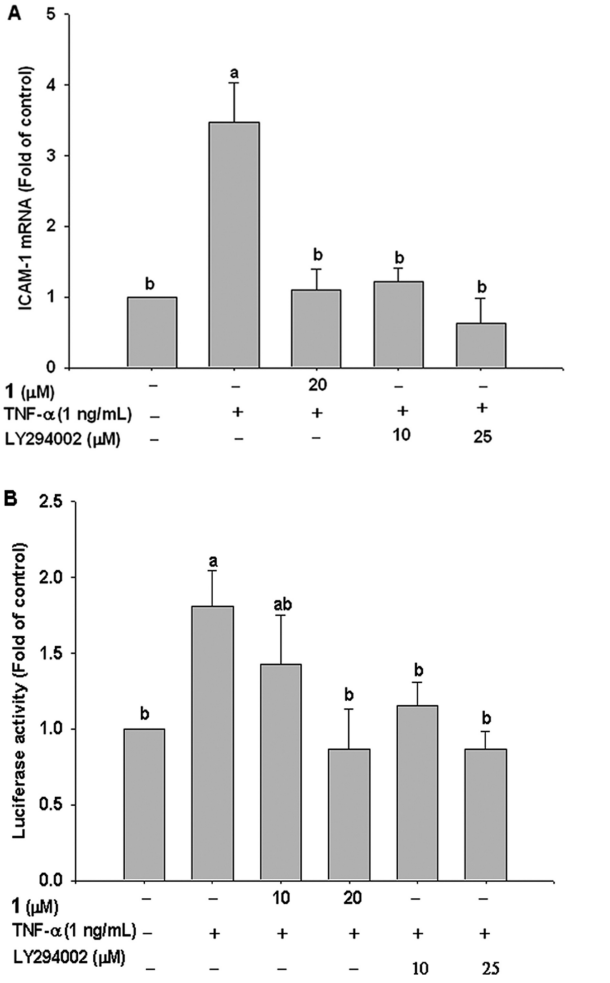

Figure 3. Effects of andrographolide (**1**) and LY294002 on ICAM-1 mRNA and promoter activity in TNF-α-stimulated HUVEC cells. Cells were pretreated with indicated concentrations of **1** and LY294002 for 16 h before being challenged with 1 ng/mL TNF-α for an additional 6 h. (A) ICAM-1 mRNA expression was measured by RT-PCR. (B) Cells were transfected transiently with pSV-β-galactosidase and human ICAM-1 promoter-Luc reporter genes for 4 h. Transfected cells were pretreated with indicated concentrations of **1** and LY294002 for 30 min before being challenged with 1 ng/mL TNF-α for an additional 5 h. Cells were harvested, and the level of luciferase and β-galactosidase activity was measured by the luciferase assay system and the β-galactosidase enzyme assay system with reporter lysis buffer (Promega Co.), respectively. Values are means ± SD of three independent experiments, and values not designated by the same letter are significantly different ($p < 0.05$).

shown by competition assays with 50-fold excess amounts of an unlabeled NF-κB probe and an unlabeled mutant NF-κB probe. When cells were treated with andrographolide (**1**) alone, no NF-κB activation was observed (data not shown).

In human pulmonary epithelial A549 cells, TNF-α activates ICAM-1 and VCAM-1 promoter activities through the NF-κB binding site rather than AP-1 and STAT binding sites.[33] Compound **1** decreases NF-κB activation, as well as ICAM-1 and E-selectin expression, in the lungs in a LPS-induced mouse model.[34] Moreover, **1** inhibits TNF-α-induced NF-κB activation in HUVEC cells and a C2C12 myotube.[35] In agreement with these studies, the results of the present experiment showed that **1** decreased TNF-α-induced ICAM-1 gene transcription and NF-κB activation in HUVEC cells. Besides inhibition of adhesion molecule expression, **1** attenuates allergic reactions in an ovalbumin-challenged asthma BALB/c mouse model and exhibits radiosensitization activity in RAS-transformed cells through inhibition of NF-κB activation.[34,36−38] Accordingly, these results indicate that regulation of the NF-κB pathway may be associated with the biological activities of **1**.

Activation of Akt in TNF-α-Stimulated HUVEC Cells by Andrographolide (1). The Akt signaling pathway is reportedly involved in TNF-α-induced up-regulation of ICAM-1 expression,[18] and expression of constitutively active Akt was sufficient to induce NF-κB activation and ICAM-1 expression.[39] Western blots probed with Akt and phosphorylated Akt antibodies were used to determine the effects of **1** on TNF-α-induced Akt activation. Akt phosphorylation increased 15 min after TNF-α treatment, and this increase reached a maximum at 60 min. Pretreatment of HUVEC cells with 20 μM **1** for 16 h reduced TNF-α-induced Akt phosphorylation

dx.doi.org/10.1021/np200631v | J. Nat. Prod. 2011, 74, 2408−2413

significantly at 15 min and later (Figure 4A). Moreover, pretreatment with the PI3K/Akt inhibitor LY294002 decreased

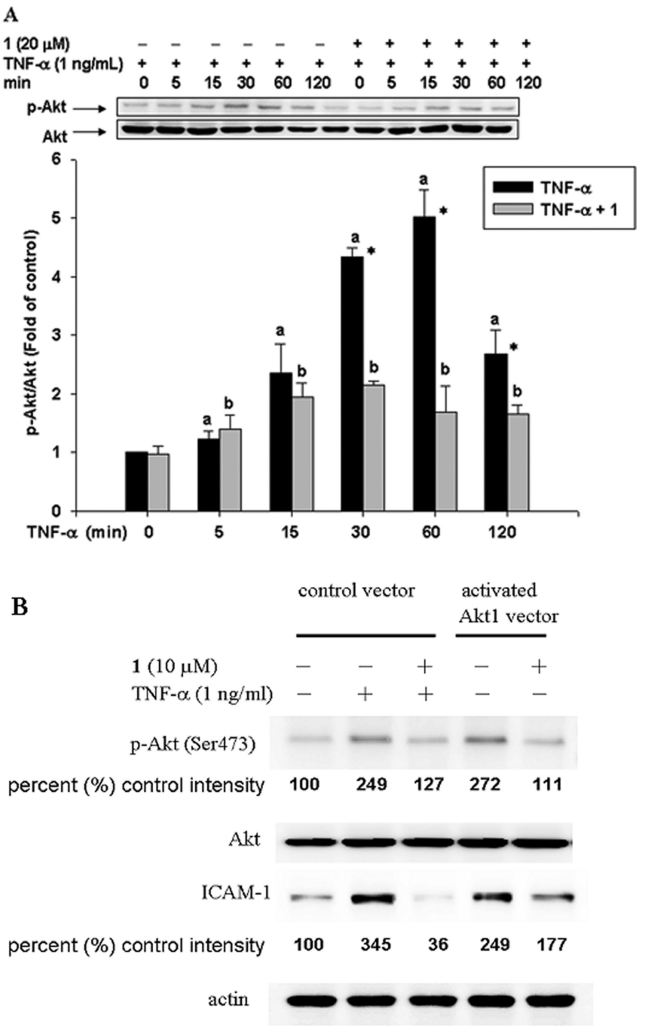

Figure 4. Effect of andrographolide (**1**) on Akt phosphorylation in TNF-α-stimulated HUVEC cells and Akt1 overexpression cells. (A) Cells were pretreated with 20 μM **1** for 16 h and then challenged with 1 ng/mL TNF-α for the indicated periods. Cells were lysed, and Western blotting was performed to phosphorylated (ser473) and total Akt protein expression. (B) Cells transfected with an empty vector or an activated Akt1 cDNA in pUSEamp were used. Cells transfected with empty vector were pretreated with 10 μM **1** for 16 h and then challenged with 1 ng/mL TNF-α for an additional 6 h. Cells transfected with an activated Akt1 cDNA in pUSEamp were incubated with 10 μM **1** for 16 h. Values are means ± SD of three independent experiments. An asterisk (*) indicates a significant difference between the mean of TNF-α alone and that of TNF-α with **1** treatment at the same time points ($p < 0.05$). Within the same treatment groups, superscripts "a" and "b", respectively, indicate significant differences ($p < 0.05$) when compared with the controls.

significantly not only ICAM-1 mRNA expression and ICAM-1 luciferase activity (Figures 3A and B) but also NF-κB activation induced by TNF-α (Figure S1C, Supporting Information). Increase of Akt phosphorylation was not noticed in cells treated with andrographolide (**1**) alone (data not shown). In order to confirm the role of Akt in the inhibition of TNF-α-induced inflammation by **1**, a genetic approach was used to constitutively activate Akt in HUVEC cells. These cells transfected with an activated Akt1 cDNA vector had increased levels of phospho-Akt and ICAM-1 expression similar to cells transfected with a control vector and treated with TNF-α (Figure 4B). Besides the inhibitory effect of **1** on ICAM-1, andrographolide (**1**) decreases MMP-7 expression through a reduction of PI3K/Akt signaling and further down-regulation of AP-1 transcriptional activity, which, in turn, results in a reduction of the migration and invasion of human non-small-cell lung cancer A549 cells.[40]

In addition to the role in HO-1 and nuclear factor erythroid 2-related factor 2,[27] the present study has indicated that improvement of vascular inflammation by **1** is at least partially attributed to inhibition of the PI3K/Akt signaling pathway and downstream target NF-κB activation in TNF-α-stimulated HUVEC cells. The findings of this study are presented schematically in Supporting Information, Figure S2. The present study has provided new insights into the possible mechanisms responsible for the potential antiatherosclerotic activity of **1**.

EXPERIMENTAL SECTION

Materials. Andrographolide (**1**) was obtained from Calbiochem (Darmstadt, Germany). The purity of andrographolide (**1**) determined by HPLC was 98%. HUVEC and monocytic HL-60 cells were obtained from Clonetics Co. (San Diego, CA, USA) and Bioresources Collection and Research Center (BCRC, Taiwan), respectively. Fetal bovine serum was from Biological Industries (Kibbutz Beit-Haemek, Israel), and medium 199 and RPMI 1640 were acquired from Gibco-BRL (Grand Island, NY, USA). Endothelial cell growth supplement was purchased from Upstate Biotechnology (Lake Placid, NY, USA), and heparin, LY294002, TNF-α, and MTT were from Sigma (St. Louis, MO, USA). The antibodies against ICAM-1 and IκB-α were purchased from Santa Cruz Biotechnology (Santa Cruz, CA, USA). The specific antibodies for total and phosphorylated Akt were from Cell Signaling Technology (Boston, MA, USA). Antibodies to p65 and β-actin were obtained from BD Biosciences (San Diego, CA, USA) and Sigma (St. Louis, MO, USA), respectively. 2′,7′-Bis(2-carboxyethyl)-5(6)-carboxyfluorescein acetoxymethyl ester (BCECF-AM) and fluorescein isothiocyanate (FITC)-conjugated goat anti-mouse ICAM-1 antibody were ordered from Molecular Probes (Eugene, OR, USA) and Serotec Company (Oxford, UK), respectively. TRIzol regent was from Invitrogen (Carlsbad, CA, USA), and BioTaq DNA polymerase was from Bioline USA, Inc. (Taunton, MA, USA). Except for Taq DNA polymerase, reagents such as enzymes, cofactors, and nucleotides for the reverse transcriptase polymerase chain reaction (RT-PCR) were from Promega Company (Madison, WI, USA). The oligonucleotide primers of ICAM-1 and glyceraldehyde-3-phosphate dehydrogenase (GAPDH) for RT-PCR as well as the biotin-labeled double-stranded NF-κB consensus oligonucleotide, nonlabeled double-stranded NF-κB consensus oligonucleotide, and a mutant double-stranded NF-κB oligonucleotide for electrophoretic mobility shift assay (EMSA) were synthesized by MDBio, Inc. (Taipei, Taiwan). The human ICAM-1 promoter luciferase plasmid (pIC339) was a gift from Dr. P. T. van der Saag (Hubrecht Laboratory, Utrecht, The Netherlands), and the luciferase reporter assay kit was from BD Biosciences. The pSV-β-galactosidase control vector and β-galactosidase enzyme assay system were from Promega. All other chemicals were of the highest quality available.

Cell Cultures. HUVEC cells of passages between 7 and 9 were used in this study. Cells were maintained in medium 199 supplemented with 20 mmol/L HEPES (pH 7.4), 30 mg/L endothelial cell growth supplement, 100 mg/L heparin, 20% fetal bovine serum, 100000 u/L penicillin, and 100 mg/L streptomycin at 37 °C under 5% CO_2. The HL-60 cells were grown in RPMI 1640 medium supplemented with 10% fetal bovine serum, 100000 u/L penicillin, and 100 mg/L streptomycin. Experiments were initiated when the HUVEC cells were at 80% confluence.

dx.doi.org/10.1021/np200631v | J. Nat. Prod. 2011, 74, 2408–2413

Cell Viability Assay. The mitochondrial-dependent reduction of MTT to formazan was used to measure cell respiration as an indicator of cell viability.[41] HUVEC cells were stimulated with TNF-α (1 ng/mL) for 6 h after pretreatment with **1** for 16 h. After treatment, cells were incubated in 199 medium containing 0.5 mg/mL of MTT for an additional 3 h. The medium was then removed, and 2-propanol was added to dissolve the formazan. After centrifugation at 5000*g* for 5 min, 100 μL of supernatant from each sample was transferred to 96-well plates, and absorbance was read at 570 nm in a VersaMax tunable microplate reader (Molecular Devices Corporation, Sunnyvale, CA, USA).

Western Blot Analysis. Cells were washed twice with cold PBS and were harvested in 150 μL of lysis buffer containing 10 mM Tris-HCl, 5 mM EDTA, 0.2 mM phenylmethylsulfonyl fluoride (PMSF), and 20 μg/mL aprotinin, pH 7.4. The protein content in each sample was quantified by use of the Coomassie Plus Protein Assay Reagent Kit (Pierce Chemical Co., Rockford, IL, USA). Equal amounts of proteins were denatured and separated on SDS-polyacrylamide gels and then transferred to polyvinylidene difluoride membranes (New Life Science Product, Inc., Boston, MA, USA). Nonspecific binding sites on the membranes were blocked with 5% nonfat dry milk in a buffer containing 10 mM Tris-HCl and 100 mM NaCl, pH 7.5, at 4 °C overnight. The blots were then incubated sequentially with primary antibody and horseradish peroxidase-conjugated anti-goat or anti-rabbit IgG (Bio-Rad, Hercules, CA, USA). Immunoreactive protein bands were developed using enhanced chemiluminescence kits (Amersham Life Sciences, Arlington Heights, IL, USA) and then were quantified through densitometric analysis by Alphalmager 2000 (Alpha Innotech, San Leandro, CA, USA).

Monocyte Adhesion Assay. A total of 1 mL of 1×10^8 HUVEC cells was plated in 24-well plates and allowed to grow to 80% confluence. At the end of treatment by andrographolide (**1**) and TNF-α, 4×10^5 BCECF-AM-labeled HL-60 cells were placed into each well, and the cells were co-incubated with HUVEC cells at 37 °C for 30 min. The wells were washed and filled with cell culture medium, and the plates were sealed, inverted, and centrifuged at 100*g* for 5 min to remove nonadherent HL-60 cells. Bound HL-60 cells were lysed in a 1% SDS solution, and the fluorescence intensity was examined using a HTS 7000 plate reader (PerkinElmer Instruments, Norwalk, CT), with an excitation wavelength of 490 nm and an emission wavelength of 520 nm. A control study showed that fluorescence is a linear function of HL-60 cells in the range 3000 to 60 000 cells/well. On the basis of the standard curve obtained, the results are reported as the number of adherent HL-60 cells per well.[42]

ICAM-1 Expression on Cell Surfaces. The effect of andrographolide (**1**) on TNF-α-induced ICAM-1 expression on the cell surface was measured by fluorescence flow cytometry. HUVEC cells were incubated with **1** for 16 h and were then stimulated with 1 ng/mL of TNF-α for an additional 6 h. After treatment, cells were detached with trypsin and centrifuged at 400*g* for 5 min. Cells were reacted with FITC-conjugated goat anti-mouse ICAM-1 antibody (Serotec, Oxford, UK) at 4 °C for 45 min in the dark. Cells were washed three times with cold PBS, resuspended in 500 μL of PBS, and immediately subjected to cytometric analysis [Becton Dickinson FACSCalibur (BD Biosciences, San Jose, CA, USA)].

RNA Isolation and RT-PCR. Total RNA was isolated from HUVEC cells using TRIzol reagent, as recommended by the manufacturer. RNA extracts were suspended in nuclease-free water and were frozen at −70 °C until RT-PCR analysis was performed. Altogether, 4 μg total RNA was used for the synthesis of first-strand cDNA with Moloney murine leukemia virus reverse transcriptase in a final volume of 20 μL containing 5 mM $MgCl_2$, 1 mM of each deoxynucleotide triphosphate, 2.5 mM oligo$(dT)_{16}$ and 40 units of RNase inhibitor. PCR was carried out in a thermocycler in a 50 μL reaction volume containing 20 μL of cDNA, BioTaq PCR buffer, 4 mM $MgCl_2$, and 2.5 units Taq polymerase, and 6 pmol forward and reverse primers. Oligonucleotide primers of ICAM-1 (forward, 5′-TGAAGGCCACCCCAGAGGACAAC-3′; reverse, 5′-CCCATTATGACTGCGGCTGCTGCTACC-3′) and GAPDH (forward, 5′-GAGTCAACGGATTTGGTCGT-3′; reverse, 5′-TTGATTTTGGAGGGATCTCG-3′) were designed on the basis of published sequences.[43] Amplification of ICAM-1 and GAPDH was achieved when samples were heated to 95 °C for 5 min and then immediately cycled 32 times through a 1 min denaturing step at 94 °C, a 1 min annealing step at 55 °C, and a 2 min elongation step at 72 °C. The GAPDH cDNA level was used as the internal standard. PCR products were resolved in a 1% agarose gel, scanned using a digital image analyzer (Alpha Innotech), and quantitated with ImageGauge.

Transient Transfection and Luciferase Assay. The control pUSEamp empty vector and an expression construct for Akt1 cDNA in pUSEamp were gifts from Dr. J. H. Chen, Chung Shan Medical University, Taichung, Taiwan. Liposome-mediated transfection was performed using Lipofectamine (Invitrogen) on HUVEC cells with a control pUSEamp empty vector or an expression construct for activated Akt1 cDNA in pUSEamp. Briefly, these cells were plated onto a 3 cm dish and transfected with the indicated plasmid at 70−80% confluence using Lipofectamine reagent, according to the manufacturer's instructions. Lipofectamine (2 μL) and DNA (1 μg) were diluted in 100 μL of OPTI medium followed by equilibration at room temperature for 10 min after mixing. The lipofectamine−DNA complex was added to HUVEC cells and incubated for 12 h. Cells were then replenished with M199 containing 20% serum and incubated for 2 h. At 14 h after transfection, the cells were incubated with 10 μM **1** for 16 h and then stimulated with 1ng/mL of TNF-α for 6 h.

The human ICAM-1 promoter luciferase plasmid (pIC339) was transfected using nanofection regent (PAA Laboratories GmbH, Pasching, Austria), according to the manufacturer's instructions. The transfected cells were treated with **1** or LY294002 for 30 min and then stimulated with 1 ng/mL of TNF-α for 5 h. Supernatants of the cell lysates were applied to measure the luciferase and β-galactosidase activities using a luciferase reporter assay kit and a β-galactosidase enzyme assay system, respectively. β-Galactosidase activity was used to normalize transfection efficacy.

Preparation of Nuclear Protein and EMSA. At the time of harvest, cells were scraped with cold PBS and centrifuged. The pellets were resuspended in the hypotonic extraction buffer (10 mM HEPES, 10 mM KCl, 1 mM $MgCl_2$, 1 mM EDTA, 0.5 mM dithiothreitol, 0.2 mM PMSF, 4 μg/mL leupeptin, 20 μg/mL aprotinin, and 0.5% NP-40) for 15 min on ice and were then centrifuged at 6000*g* for 15 min. The pelleted nuclei were resuspended in 50 μL of hypertonic extraction buffer (10 mM HEPES, 400 mM KCl, 1 mM $MgCl_2$, 1 mM EDTA, 0.5 mM dithiothreitol, 0.2 mM PMSF, 4 μg/mL leupeptin, 20 μg/mL aprotinin, and 10% glycerol), constantly shaken at 4 °C for 30 min, and then centrifuged at 10000*g* for 15 min. The resultant supernatants containing nuclear proteins were collected and stored at −70 °C until EMSA was performed.

EMSA was performed according to a previous study.[44] The LightShift chemiluminescent EMSA kit (Pierce Chemical Co.) and synthetic biotin-labeled double-stranded NF-κB consensus oligonucleotide (5′-AGTTGAGGGGACTTTCCCAGGC-3′) were used to measure the effect of **1** on NF-κB nuclear protein−DNA binding activity. Nuclear proteins (2 μg), poly(dI-dC), and biotin-labeled double-stranded NF-κB oligonucleotide were mixed with the binding buffer to a final volume of 20 μL and incubated at room temperature for 30 min. In addition, an excess amount (100-fold molar excess) of unlabeled and a mutant double-stranded NF-κB oligonucleotide (5′-AGTTGAGG$_{\underline{C}}$GACTTTCCCAGGC-3′) were used for the competition assay to confirm specificity of binding. The nuclear protein−DNA complex was separated by electrophoresis on a 6% tris/boric acid/EDTA-polyacrylamide gel and was then electrotransfered to a nylon membrane (HybondTM-N+, Amersham Pharmacia Biotech Inc., Piscataway, NJ). The membrane was treated with streptavidin-horseradish peroxidase, and the nuclear protein−DNA bands were developed by using a SuperSignal West Pico kit (Pierce Chemical Co.).

Statistical Analysis. Data are expressed as the means ± SD from three independent experiments. Statistically significant differences were analyzed by Student's *t* test or ANOVA and Tukey's multiple-

range test by using the Statistical Analysis System (Cary, NC). p values less than 0.05 were considered to be significant.

■ ASSOCIATED CONTENT

Supporting Information

Effects of andrographolide (**1**) on NF-κB activation in TNF-α-stimulated HUVEC cells and diagram summarizing the molecular mechanism underlying the andrographolide (**1**) inhibition of inflammation. This material is available free of charge via the Internet at http://pubs.acs.org.

■ AUTHOR INFORMATION

Corresponding Author

*Tel: +886-4-22053366, ext. 7519. Fax: +886-4-22062891. E-mail: cklii@mail.cmu.edu.tw (C.K.L.). Tel: +886-4-24730022, ext. 12205. E-mail: kaililiu@csmu.edu.tw (K.L.L.).

■ ACKNOWLEDGMENTS

This work was supported by Grant CMU99-ASIA-09.

■ REFERENCES

(1) Sfikakis, P. P. *Curr. Dir. Autoimmun.* **2010**, *11*, 180−210.
(2) Fujiwara, N.; Kobayashi, K. *Curr. Drug Targets Inflamm. Allergy* **2005**, *4*, 281−286.
(3) Otto, B. A.; Wenzel, S. E. *Curr. Opin. Otolaryngol. Head Neck Surg.* **2008**, *16*, 270−274.
(4) Krieglstein, C. F.; Granger, D. N. *Am. J. Hypertens.* **2001**, *14*, 44S−54S.
(5) van de Stolpe, A.; van der Saag, P. T. *J. Mol. Med.* **1996**, *74*, 13−33.
(6) Collins, R. G.; Velji, R.; Guevara, N. V.; Hicks, M. J.; Chan, L.; Beaudet, A. L. *J. Exp. Med.* **2000**, *191*, 189−194.
(7) Ballantyne, C. M. *Am. J. Manag. Care* **2001**, *7* (5 Suppl), S144−S147.
(8) Ledebur, H. C.; Parks, T. P. *J. Biol. Chem.* **1995**, *270*, 933−943.
(9) Chen, C. C.; Rosenbloom, C. L.; Anderson, D. C.; Manning, A. M. *J. Immunol.* **1995**, *155*, 3538−3545.
(10) Baldwin, A. S. Jr. *Annu. Rev. Immunol.* **1996**, *14*, 649−683.
(11) Hayden, M. S.; Ghosh, S. *Genes Dev.* **2004**, *18*, 2195−2224.
(12) Lawrence, T. *Cold Spring Harb. Perspect. Biol.* **2009**, *1*, a001651.
(13) Brand, K.; Page, S.; Rogler, G.; Bartsch, A.; Brandl, R.; Knuechel, R.; Page, M.; Kaltschmidt, C.; Baeuerle, P. A.; Neumeier, D. *J. Clin. Invest.* **1996**, *97*, 1715−1722.
(14) Collins, T.; Cybulsky, M. I. *J. Clin. Invest.* **2001**, *107*, 255−264.
(15) Hennessy, B. T.; Smith, D. L.; Ram, P. T.; Lu, Y.; Mills, G. B. *Nat. Rev. Drug Discovery* **2005**, *4*, 988−1004.
(16) Ozes, O. N.; Mayo, L. D.; Gustin, J. A.; Pfeffer, S. R.; Pfeffer, L. M.; Donner, D. B. *Nature* **1999**, *401*, 82−85.
(17) Gerszten, R. E.; Friedrich, E. B.; Matsui, T.; Hung, R. R.; Li, L.; Force, T.; Rosenzweig, A. *J. Biol. Chem.* **2001**, *276*, 26846−26851.
(18) Dagia, N. M.; Agarwal, G.; Kamath, D. V.; Chetrapal-Kunwar, A.; Gupte, R. D.; Jadhav, M. G.; Dadarkar, S. S.; Trivedi, J.; Kulkarni-Almeida, A. A.; Kharas, F.; Fonseca, L. C.; Kumar, S.; Bhonde, M. R. *Am. J. Physiol. Cell Physiol.* **2010**, *298*, C929−C941.
(19) Kim, H. G.; Kim, J. Y.; Hwang, Y. P.; Lee, K. J.; Lee, K. Y.; Kim, D. H.; Kim, D. H.; Jeong, H. G. *Toxicol. Appl. Pharmacol.* **2006**, *217*, 332−341.
(20) Lii, C. K.; Lei, Y. P.; Yao, H. T.; Hsieh, Y. S.; Tsai, C. W.; Liu, K. L.; Chen, H. W. *J. Ethnopharmacol.* **2010**, *128*, 213−220.
(21) Parasher, P.; Upadhyay, A.; Khan, N. A.; Dwivedi, S. K. *Electron. J. Environ. Agric. Food Chem.* **2011**, *10*, 2479−2486.
(22) Roxas, M.; Jurenka, J. *Altern. Med. Rev.* **2007**, *12*, 25−48.
(23) Chao, W. W.; Kuo, Y. H.; Li, W. C.; Lin, B. F. *J. Ethnopharmacol.* **2009**, *122*, 68−75.
(24) Chiou, W. F.; Chen, C. F.; Lin, J. J. *Br. J. Pharmacol.* **2000**, *129*, 1553−1560.
(25) Hansson, G. K. *J. Thromb. Haemost.* **2009**, *7* (Suppl 1), 328−331.
(26) Patel, S.; Celermajer, D. S.; Bao, S. *Int. J. Biochem. Cell Biol.* **2008**, *40*, 576−580.
(27) Yu, A. L.; Lu, C. Y.; Wang, T. S.; Tsai, C. W.; Liu, K. L.; Cheng, Y. P.; Chang, H. C.; Lii, C. K.; Chen, H. W. *J. Agric. Food Chem.* **2010**, *58*, 7641−7648.
(28) Habtemariam, S. *Phytother. Res.* **1998**, *12*, 37−40.
(29) Blankenberg, S.; Barbaux, S.; Tiret, L. *Atherosclerosis* **2003**, *170*, 191−203.
(30) Hsieh, C. Y.; Hsu, M. J.; Hsiao, G.; Wang, Y. H.; Huang, C. W.; Chen, S. W.; Jayakumar., T.; Chiu, P. T.; Chiu, Y. H.; Sheu, J. R. *J. Chem. Biol.* **2011**, *286*, 5942−5955.
(31) Kevil, C. G.; Patel, R. P.; Bullard, D. C. *Am. J. Physiol. Cell Physiol.* **2001**, *281*, C1442−C1447.
(32) Kang, J. S.; Yoon, Y. D.; Han, M. H.; Han, S. B.; Lee, K.; Lee, K. H.; Park, S. K.; Kim, H. M. *Mol. Pharmacol.* **2006**, *69*, 941−949.
(33) Oh, J. H.; Park, E. J.; Park, J. W.; Lee, J.; Lee, S. H.; Kwon, T. K. *Int. Immunopharmacol.* **2010**, *10*, 572−579.
(34) Xia, Y. F.; Ye, B. Q.; Li, Y. D.; Wang, J. G.; He, X. J.; Lin, X.; Yao, X.; Ma, D.; Slungaard, A.; Hebbel, R. P.; Key, N. S.; Geng, J. G. *J. Immunol.* **2004**, *173*, 4207−4217.
(35) Jackman, R. W.; Rhoads, M. G.; Cornwell, E.; Kandarian, S. C. *Exp. Cell Res.* **2009**, *315*, 3242−3249.
(36) Bao, Z.; Guan, S.; Cheng, C.; Wu, S.; Wong, S. H.; Kemeny, D. M.; Leung, B. P.; Wong, W. S. *Am. J. Respir. Crit. Care Med.* **2009**, *179*, 657−665.
(37) Li, J.; Luo, L.; Wang, X.; Liao, B.; Li, G. *Cell Mol. Immunol.* **2009**, *6*, 381−385.
(38) Hung, S. K.; Hung, L. C.; Kuo, C. D.; Lee, K. Y.; Lee, M. S.; Lin, H. Y.; Chen, Y. J.; Fu, S. L. *Int. J. Radiat. Oncol. Biol. Phys.* **2010**, *77*, 1232−1239.
(39) Minhajuddin, M.; Bijli, K. M.; Fazal, F.; Sassano, A.; Nakayama, K. I.; Hay, N.; Platanias, L. C.; Rahman, A. *J. Biol. Chem.* **2009**, *284*, 4052−4061.
(40) Lee, Y. C.; Lin, H. H.; Hsu, C. H.; Wang, C. J.; Chiang, T. A.; Chen, J. H. *Eur. J. Pharmacol.* **2010**, *632*, 23−32.
(41) Denizot, F.; Lang, R. *J. Immunol. Methods* **1986**, *89*, 271−277.
(42) Yoshida, M.; Chien, L. J.; Yasukochi, Y.; Numano, F. *Ann. N.Y. Acad. Sci.* **2000**, *902*, 307−310.
(43) Meagher, L.; Mahiouz, D.; Sugars, K.; Burrows, N.; Norris, P.; Yarwood, H.; Becker-Andre, M.; Haskard, D. O. *J. Immunol. Methods* **1994**, *175*, 237−246.
(44) Cheng, W. L.; Lii, C. K.; Chen, H. W.; Lin, T. H.; Liu, K. L. *J. Agric. Food Chem.* **2004**, *52*, 71−78.